

# The hepatitis C virus p7 protein forms an ion channel that is inhibited by long-alkyl-chain iminosugar derivatives

Davor Pavlović\*, David C. A. Neville\*, Olivier Argaud\*, Baruch Blumberg†, Raymond A. Dwek\*, Wolfgang B. Fischer\*, and Nicole Zitzmann\*\*

\*Department of Biochemistry, University of Oxford, Oxford OX1 3QU, United Kingdom; and †Fox Chase Cancer Center, Philadelphia, PA 19111

Contributed by Baruch Blumberg, March 17, 2003

**We show that hepatitis C virus (HCV) p7 protein forms ion channels in black lipid membranes. HCV p7 ion channels are inhibited by long-alkyl-chain iminosugar derivatives, which have antiviral activity against the HCV surrogate bovine viral diarrhea virus. HCV p7 presents a potential target for antiviral therapy.**

Hepatitis C virus (HCV) is the major cause of chronic hepatitis with a significant risk of end-stage liver cirrhosis and hepatocellular carcinoma (1). HCV belongs to the family *Flaviviridae*, which consists of three genera: flaviviruses, pestiviruses, and hepaciviruses. In the absence of both a suitable small animal model and a reliable *in vitro* infectivity assay for HCV, potential antiviral drugs initially have been tested by using a related pestivirus, bovine viral diarrhea virus (BVDV) (2). BVDV *in vitro* infectivity assays were used to demonstrate that long-alkyl-chain iminosugar derivatives containing either the glucose analogue deoxynojirimycin (DNJ) or the galactose analogue deoxygalactonojirimycin (DGJ) are potent antiviral inhibitors (3).

DNJ derivatives inhibit endoplasmic reticulum (ER)  $\alpha$ -glucosidases I and II (4, 5), and this inhibition leads to the misfolding of many host- and virus-encoded glycoproteins, including the envelope glycoproteins of BVDV (6) and HCV (7). Previous experiments have shown that the antiviral effect of the long-alkyl-chain derivative *N*-nonyl-DNJ (NN-DNJ) is more pronounced than that of the short-alkyl-chain derivative *N*-butyl-DNJ (NB-DNJ), although the latter achieves a more effective ER  $\alpha$ -glucosidase inhibition *in cellulose*. In addition, long-alkyl-chain DGJ derivatives that are not recognized by and do not inhibit ER  $\alpha$ -glucosidases also show potent antiviral activity (3). Therefore, ER  $\alpha$ -glucosidase inhibition does not correlate directly with the observed antiviral effect and is ruled out as the sole antiviral mechanism.

The additional mechanism of action apparently is associated with the length of the alkyl side chain, because the short-chain *N*-butyl-DGJ (NB-DGJ) shows no antiviral activity, whereas the long-alkyl-chain derivative NN-DGJ is a potent inhibitor (3).

The predominant antiviral mechanism is proposed to be mediated directly or indirectly by an effect of the long-alkyl side chains on the membrane and/or membrane proteins, because treatment with long-alkyl-chain iminosugars affects the dimerization of viral membrane glycoproteins and alters the membrane glycoprotein composition of secreted BVDV virions but does not influence either viral RNA replication or protein synthesis (3).

We decided to investigate the small membrane-spanning protein p7 as a potential target of long-alkyl-chain iminosugar derivatives, because flaviviruses such as dengue virus and Japanese encephalitis virus (8), which do not contain p7, are not inhibited by long-alkyl-chain DGJ derivatives, whereas pestiviruses are (3). Pesti- and hepaciviruses both contain the p7 protein.

Most functional data about p7 are derived from the pestivirus p7, a 70-aa protein very similar to HCV p7. Functional

data have been obtained by introducing mutations into an infectious cDNA clone of BVDV. An in-frame deletion of the entire p7 does not affect RNA replication but leads to the production of noninfectious virions. However, infective viral particles can be generated by complementing p7 in trans (9), which suggests that the pestivirus p7 is essential for the production of infective progeny virus. Interestingly, noninfective BVDV particles also are created by treatment with long-alkyl-chain iminosugar derivatives (3).

Recently, HCV p7 has been shown to be a polytopic membrane protein that crosses the membrane twice and has its N and C termini oriented toward the extracellular environment (10). Subgenomic replicon studies have shown that the p7 of HCV is not necessary for genome replication (11, 12), and its role in infectious virus production remains unknown. HCV p7 has been suggested by Harada *et al.* (9) and Carrère-Kremer *et al.* (10) to be a member of a group of small proteins known as viroporins (13), which mediate cation permeability across membranes and are important for virion release or maturation. In this report, we show that by using an artificial lipid bilayer system, chemically synthesized HCV p7 protein forms ion channels in black lipid membranes (BLM). Furthermore, long-alkyl-chain iminosugar derivatives, which are antiviral against BVDV, suppress HCV p7 ion channel signals.

## Materials and Methods

**Peptide Synthesis and Product Quality Control.** Fifty milligrams of the peptide corresponding to p7 (HCV H strain) with a biotin tag added at the N terminus, biotin-ALENLVILNAA-SLAGTHGLVSLVFFCFAWYLKGRWVPGAVYAFYGM-WPLLLLLLALPQRAYA, was synthesized by Albachem (Edinburgh). The p7 peptide was analyzed by matrix-assisted laser desorption ionization mass spectrometry and Tris/Tricine (Tris/*N*-[tris(hydroxymethyl)methyl]glycine) gel electrophoresis, using a modified version of the method developed by Schägger and von Jagow (14). The gels were analyzed by both silver staining and Western blotting. For Western blot analysis, the protein from the gel was transferred to an Immobilon P membrane (Amersham Pharmacia) by using a semidry electroblotter (Merck), probed with horseradish peroxidase-coupled streptavidin, and developed by using the enhanced chemiluminescence detection system (Amersham Pharmacia), following the manufacturer's instructions.

**Channel Recordings in BLM.** A BLM was formed across an elliptical aperture of  $\approx 100\text{-}\mu\text{m}$  diameter on the long axis in a thin Teflon film (thickness,  $\approx 25\ \mu\text{m}$ ; Yellow Springs Instruments) (15). Forty microliters of a mixture of lipids [1-palmitoyl-2-oleoyl-*sn*-

Abbreviations: HCV, hepatitis C virus; BVDV, bovine viral diarrhea virus; DNJ, deoxynojirimycin; DGJ, deoxygalactonojirimycin; NN-DNJ, *N*-nonyl-DNJ; NB-DNJ, *N*-butyl-DNJ; Tricine, *N*-[tris(hydroxymethyl)methyl]glycine; BLM, black lipid membranes.

\*To whom correspondence should be addressed. E-mail: nic@oxglua.glycobioc.ox.ac.uk.

glycero-3-phosphoethanolamine/1-palmitoyl-2-oleoyl-*sn*-glycero-3-phosphocholine (4:1, wt/wt)] was dissolved in pentane (5 mg/ml) and spread on top of an aqueous subphase (0.5 M KCl/5 mM Hepes/1 mM CaCl<sub>2</sub>, pH 7.4). This resulted in ≈0.2 mg of lipid on each side of the thin Teflon film. A time period of 10 min was allowed for the solvent to evaporate before the BLM was formed by raising the buffer level across the hole in the Teflon film. After formation of a stable BLM, the HCV p7 protein (dissolved in ethanol) was added from a 200-fold excess stock solution to the aqueous subphase (volume in each chamber on both sides of the bilayer: 2 ml) of the (electrically grounded) trans side to reach a final concentration of ≈50 μM. Recordings appeared after a time delay of ≈10 min. Electrical currents were recorded with an Axopatch 1D amplifier at 5 kHz. Data were filtered by using a cut-off frequency of 50 Hz and analyzed further by using the software ORIGIN 5.0. Iminosugar derivatives [from 10 mM stock solutions of *NN*-DNJ (provided by Synergy Pharmaceuticals, Somerset, NJ), *NN*-DGJ (purchased from Toronto Research Chemicals, Downsview, ON, Canada), and *N*-7-oxanonyl-6-deoxy-DGJ (supplied by United Therapeutics, Silver Spring, MD) and from 100 mM stock solutions of *NB*-DNJ (Sigma) and *NB*-DGJ (synthesized in-house) were added on either the cis or trans side to result in the lowest chamber concentrations stated in the figures. Increasing drug concentrations were achieved by sequential addition of equivalent volumes to the measurement chamber. Data recording started ≈1 min after the addition of drug for ≈3 min at +100 mV or +130 mV, as stated in the figure legends.

## Results

**HCV p7 Chemical Synthesis and Product Analysis.** A biotin-tagged version of p7 (HCV H strain) was synthesized chemically (biotin-AL<sub>1</sub>ENLVILNAASLAGTHGLV<sub>2</sub>SFLVFFCFAWYLKGRWVPGAVYALYGMWPLLLLLLALPQRAYA). After matrix-assisted laser desorption ionization mass spectrometry analysis, a peak at a *m/z* ratio of 7,247.8 corresponding to the full-length p7 peptide was observed, together with some peaks of lower *m/z* ratio (data not shown). Because of the highly hydrophobic nature and size of the full-length p7, its ionization capability is expected to be low compared with the smaller *m/z* species. Therefore, no assessment of peptide purity could be derived from the MS data. To assess the ratio of the full-length peptide to smaller, p7-derived peptides, synthetic HCV p7 was analyzed by Tris/Tricine gel electrophoresis followed by both silver staining and Western blot analysis, using streptavidin to visualize biotinylated p7. Both the silver-stained gel and the Western blot revealed one major species of the expected molecular mass when the samples were analyzed in the presence of urea. However, major differences in resolution between gels with and without urea have been observed before. The B chain of insulin (3.5 kDa), for example, migrates like a 7-kDa protein in gels with urea (14). Chemically synthesized p7 therefore was reanalyzed in the absence of urea. Whereas the streptavidin-probed Western blot revealed the presence of full-length biotinylated p7, an additional broad band of around half the apparent molecular mass was observed on silver-stained gels, which constituted between 50% and 60% of total p7 (data not shown). This broad band represents the smaller, nonbiotinylated, p7-derived species observed by MS, the masses of which theoretically correspond to fragments of p7 containing the N-terminal transmembrane domain. Because the separation of full-length p7 from truncated forms of p7 proved to be difficult, the whole preparation subsequently was used for channel recordings in BLM.

**Channel Recordings of HCV p7 in BLM.** Reconstitution of p7 into a stable BLM leads to the formation of channels. In 15 of 50 experiments in which bilayers were exposed to p7, currents such

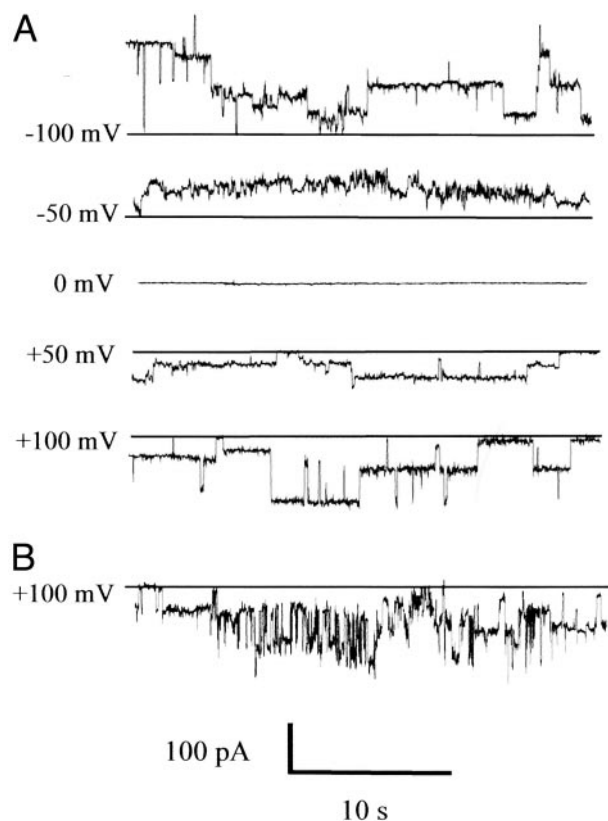


**Fig. 1.** (A) Channel recordings of synthetic HCV p7 inserted into a BLM. Channel activity is shown for ±100 mV. The closed state is shown as a solid line. Openings are deviations from this line. Solutions are the same in cis and trans: 0.5 M KCl/5 mM Hepes/1 mM CaCl<sub>2</sub>, pH 7.4. p7 is added on the trans side to a final concentration of ≈50 μM. (B) Current trace recorded after ≈30 min of data collection. Scale bars are 10 s and 100 pA.

as those shown in Fig. 1A were seen, with conductance levels of up to 2 nS at −100 mV (Fig. 1A). The smallest mean conductance level detected is  $86 \pm 22$  pS at +50 mV. The lifetime of defined conductance levels ranges from hundreds of milliseconds to several seconds. Stable, long-lasting conductance states differ by ≈100 pS (and multiples of it), suggesting the formation of a fairly stable channel with a conductance of around 100 pS. Fluctuation in the recording may indicate the presence of subconductance states. Prolonged measurements with the same sample result in increasing noise levels that eventually rule out the assignment of defined conductance levels (Fig. 1B). In 35 of 50 experiments, insertion of p7 into the BLM results in burst-like activity (e.g., Fig. 2). The solvent ethanol also was tested and showed no effect (data not shown).

### Inhibition of p7 Channels by Long-Alkyl-Chain Iminosugar Derivatives.

We applied increasing concentrations of iminosugar derivatives to one side of the membrane and followed their effect on p7-induced channel activity. With the short-alkyl-chain derivatives *NB*-DGJ (data not shown) and *NB*-DNJ, p7 channel activity remains unchanged (Fig. 2 Top). However, addition of increasing amounts of the long-alkyl-chain derivatives *NN*-DGJ, *NN*-DNJ, and *N*-7-oxanonyl-6-deoxy-DGJ leads to a dose-dependent inhibition of p7 channel signals (Figs. 2 Middle and Bottom and 3). From graphical representations of the resulting integrated normalized current traces and their respective sigmoidal fits (data not shown), we deduce approximate mean binding constants  $\pm$  SE ( $n = 3$ ) of  $K_{app} = 110.4 (\pm 19.9)$  μM for *NN*-DGJ,  $K_{app} = 45.2 (\pm 10.7)$  μM for *NN*-DNJ, and  $K_{app} = 114.2 (\pm 18.3)$  μM for

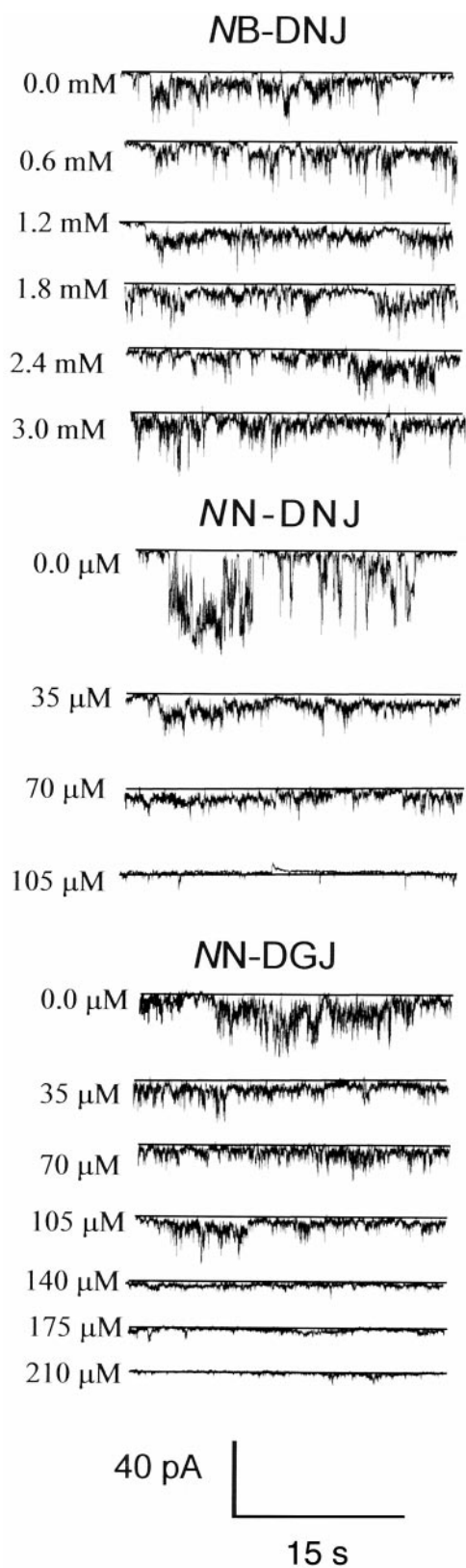


**Fig. 2.** Effect of short- and long-alkyl-chain iminosugar derivatives on p7 channel signals in BLM. The closed state is shown as a solid line. Openings are deviations from this line. Scale bars are 15 s and 40 pA. Solutions are the same in cis and trans: 0.5 M KCl/5 mM HEPES/1 mM CaCl<sub>2</sub>, pH 7.4. p7 is added on the trans side to a final concentration of  $\approx 50 \mu\text{M}$ . Compounds were added at a constant holding potential of +100 mV on the cis side to the final concentrations indicated at the left side of each recording.

## N-7-oxanonyl-6-deoxy-DGJ

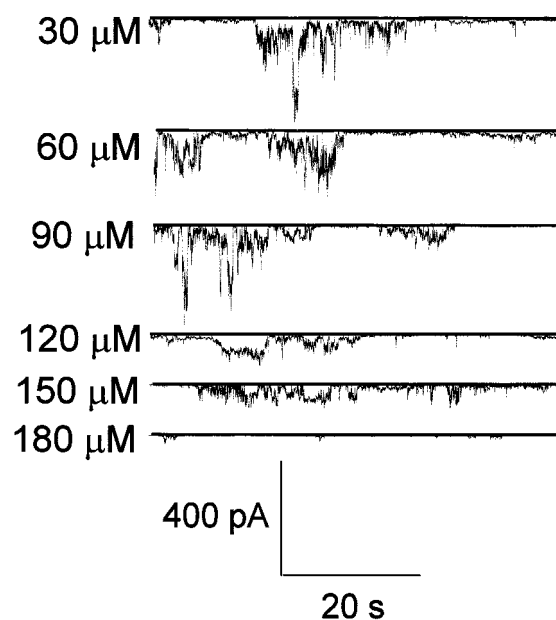


**Fig. 3.** Effect of *N*-7-oxanonyl-6-deoxy-DGJ on p7 channel signals in BLM. The closed state is shown as a solid line. Openings are deviations from this line. Scale bars are 20 s and 400 pA. Solutions are the same in cis and trans: 0.5 M KCl/5 mM HEPES/1 mM CaCl<sub>2</sub>, pH 7.4. p7 is added on the trans side to a final concentration of  $\approx 50 \mu\text{M}$ . *N*-7-oxanonyl-6-deoxy-DGJ was added at a constant holding potential of +130 mV on the trans side to the final concentrations indicated at the left side of each recording.

*N*-7-oxanonyl-6-deoxy-DGJ. Complete blockage of channel activity is observed at about 140  $\mu\text{M}$  for NN-DGJ, 105  $\mu\text{M}$  for NN-DNJ, and 180  $\mu\text{M}$  for *N*-7-oxanonyl-6-deoxy-DGJ. Drug solutions and solvent alone had no effect on the bilayer (data not shown). No leak currents were observed with increasing concentrations of any of the iminosugar derivatives.

### Discussion

N-terminally biotin-tagged full-length peptide was synthesized chemically and analyzed by matrix-assisted laser desorption ionization mass spectrometry and Tris/Tricine gel electrophoresis. P7 on Tricine gels was either silver-stained or transferred to a membrane, which subsequently was probed with streptavidin. Full-length p7 was detected on silver-stained gels and Western blots and constituted  $\approx 50\%$  of total peptide present. The peptides of lower molecular mass detected by matrix-assisted laser desorption ionization mass spectrometry could be resolved by Tris/Tricine gel electrophoresis only when urea was omitted from the samples. These species were not visible on streptavidin-stained Western blots, indicating that they are not biotin-tagged. They are either synthesis artifacts or degradation products with masses theoretically corresponding to peptides containing the N-terminal transmembrane domain 1 of p7. The length of some of these peptides could enable them to span the membrane once, and, therefore, they potentially could form pores either by themselves or by interacting with full-length p7. The extent to which this may have happened can be investigated by using nonbiotinylated, biologically produced p7. However, applying chemically synthesized transmembrane domain 1 alone to the BLM did not result in any ion channel recordings (data not shown).

HCV p7 inserted into BLM led to the formation of ion channels with a conductance of  $\approx 100$  pS. The smallest conductance level resolved in our recordings, and differences between conductance states of  $\approx 100$  pS, are in the same range of conductance values measured at the same bath electrolyte concentration of 0.5 M potassium chloride for channel-forming peptides such as  $\delta$ -toxins (16), alamethicin (17), and other channel tunnels (18). The values we observed are slightly higher than the conductance levels of  $\leq 50$  pS observed for ion channels recorded in a 0.1 M electrolyte solution (19–22). NB and Vpu, ion channel-forming proteins of influenza B virus and HIV-1, respectively, generate similar conductances of  $\approx 50$  pS and less (23–25). Membrane-spanning domains inserted into lipid bilayers also give rise to similar conductance levels (24, 26–28). Vpr, another HIV-1 auxiliary protein, induces channel activity when inserted in lipid bilayers (29). In this case, activity occurs in bursts with conductance levels between 20 and 100 pS. Conductance levels of the 6,000-Da protein encoded by  $\alpha$ -viruses cover a range from  $\approx 50$  pS to  $\approx 800$  pS (30). Other viral ion channels such as the tetrameric proton channel M2 from influenza A virus (31, 32) exhibit conductance levels in the femtoSiemen range (33, 34). Channel-forming peptides show conductance levels as high as the ones we observed for HCV p7 when five or more transmembrane helices assemble to form a pore (26, 27). We therefore conclude that (provided only one of p7's two transmembrane domains is involved in forming the actual pore) p7 needs to form at least a pentamer to account for the conductance levels observed. This conclusion is in agreement with the observation of a hexameric form of p7 when the protein was expressed in HepG2 cells and stabilized by cross-linking reagent and also with the formation of six subunits containing ring structures by GST-p7 fusion proteins observed by transmission electron microscopy (35).

The increasing noise levels observed in some of the experiments are assumed to result from a nonideal portion of p7 being inserted into the membrane, and the concentration of p7 in the membrane may vary within the time frame of a single experiment, e.g., because of p7 diffusion between the aqueous solution and the lipid layer covering the Teflon aperture. Similar noise levels in recordings of channel tunnels inserted into BLM have been observed at negative membrane potential and low electrolyte concentration (18).

Structural information about potential covalent links within the peptide or between individual p7 molecules that would stabilize a particular secondary, tertiary, or quaternary structure currently is not available. Overall, the observed pattern of the p7 channel recordings may be due to (i) an increasing or changing number of p7 peptides involved in pore formation, (ii) structural rearrangements of p7 molecules within a formed pore, and/or (iii) the presence of multiple pores in the BLM.

Treatment with long-alkyl-chain iminosugar derivatives leads to a concentration-dependent inhibition of p7 channel activity. Complete blockage of channel activity is observed at about  $140 \mu\text{M}$  for NN-DGJ,  $105 \mu\text{M}$  for NN-DNJ, and  $180 \mu\text{M}$  for *N*-7-oxanonyl-6-deoxy-DGJ, i.e., at concentrations that are in about the same range as that of other known viral channel blockers.

For example,  $5 \mu\text{M}$  amantadine totally blocks the M2 channel of influenza A virus *in vivo* (36), whereas  $20 \mu\text{M}$  is needed to reversibly block a channel made of synthetic peptides corresponding to the

transmembrane segment of M2 inserted into a BLM (37). To block an artificially reconstituted channel of either full-length NB protein of influenza B virus (25) or a channel made of peptides covering only the transmembrane domain of NB (38), the concentrations of amantadine needed are one order of magnitude higher, in the millimolar range. Amantadine is used as an antiviral drug against influenza A but not against influenza B virus.

Although we calculated approximate mean binding constants  $\pm$  SE ( $n = 3$ ) of  $K_{\text{app}} = 110.4 (\pm 19.9) \mu\text{M}$  for NN-DGJ,  $K_{\text{app}} = 45.2 (\pm 10.7) \mu\text{M}$  for NN-DNJ, and  $K_{\text{app}} = 114.2 (\pm 18.3) \mu\text{M}$  for *N*-7-oxanonyl-6-deoxy-DGJ, the actual nature of the interaction between the antiviral drugs and p7 remains to be identified. When added in *cis* instead of in *trans*, higher concentrations of *N*-7-oxanonyl-6-deoxy-DGJ were required to achieve the same inhibitory effect. This might be an indication of a preferred topology of p7 inserted in the membrane, which, consequently, would lead to energetically distinct putative binding sites.

Long-alkyl-chain iminosugars could interact directly with p7 molecules and either block the open channel or prevent the ion channels from forming and/or opening. Alternatively, the accumulation of these compounds in the membrane bilayer may indirectly prevent p7 molecules from assembling into channel-forming pores by changing membrane characteristics such as, for example, fluidity. The p7 channel inhibition by iminosugar derivatives therefore could be either direct or indirect. However, the presence in the BLM of just any compound carrying alkyl side chains of similar length, e.g., *n*-octyl glucoside, is not sufficient to achieve the same inhibitory effect on ion channels formed by p7 channels (data not shown), which favors the notion of a direct interaction of iminosugars with p7.

Our previous finding that treatment with long-alkyl-chain DGJ derivatives leads to secretion of noninfectious BVDV virions (3) phenotypically resembles the findings by Harada *et al.* (9), which show that deletion of p7 in an infectious BVDV cDNA clone does not inhibit secretion but leads to the secretion of noninfectious virions. Although the role of p7 during the virus life cycle has not yet been elucidated, the data presented here are further indication of p7 presenting a potential target for antiviral drug therapy. P7 channel inhibitors could add a more virus-specific component to the combination therapy currently used against HCV infection, which consists of PEG-conjugated IFN $\alpha$  and the nucleoside analogue ribavirin. P7 is conserved among all HCV genotypes, and an increased response rate, especially against IFN-resistant genotype 1b, would be anticipated.

The iminosugar derivative *N*-7-oxanonyl-6-deoxy-DGJ shows a very low toxicity profile in mice, rats, dogs, and monkeys (unpublished data), and side effects observed with some DNJ-based compounds caused by glucose-metabolizing enzymes recognizing and binding to DNJ are avoided (39). *N*-7-oxanonyl-6-deoxy-DGJ was entered into phase 1 clinical studies in July 2002.

We thank Drs. D. Durantel, T. D. Butters, S. Woodhouse, and D. Patil for their various and valuable help and Prof. D. Harvey for MS support. W.B.F. thanks the Abraham Research Fund (Oxford) for financial support and Prof. A. Watts (Oxford) for providing laboratory space to conduct the artificial bilayer experiments. N.Z. is a Dorothy Hodgkin Fellow of The Royal Society and a Research Fellow of Wolfson College, Oxford. This work was supported by United Therapeutics and the Oxford Glycobiology Institute Endowment.

- Di Bisceglie, A. M. (1997) *Hepatology* **26**, 34S–38S.
- Zitzmann, N., Mehta, A. S., Carrouee, S., Butters, T. D., Platt, F. M., McCauley, J., Blumberg, B. S., Dwek, R. A. & Block, T. M. (1999) *Proc. Natl. Acad. Sci. USA* **96**, 11878–11882.
- Durantel, D., Branza-Nichita, N., Carrouee-Durantel, S., Butters, T. D., Dwek, R. A. & Zitzmann, N. (2001) *J. Virol.* **75**, 8987–8998.
- Bergeron, J. J., Brenner, M. B., Thomas, D. Y. & Williams, D. B. (1994) *Trends Biochem. Sci.* **19**, 124–128.

- Peterson, J. R., Ora, A., Van, P. N. & Helenius, A. (1995) *Mol. Biol. Cell* **6**, 1173–1184.
- Branza-Nichita, N., Durantel, D., Carrouee-Durantel, S., Dwek, R. A. & Zitzmann, N. (2001) *J. Virol.* **75**, 3527–3536.
- Choukhi, A., Ung, S., Wychowski, C. & Dubuisson, J. (1998) *J. Virol.* **72**, 3851–3858.
- Wu, S. F., Lee, C. J., Liao, C. L., Dwek, R. A., Zitzmann, N. & Lin, Y. L. (2002) *J. Virol.* **76**, 3596–3604.

9. Harada, T., Tautz, N. & Thiel, H. J. (2000) *J. Virol.* **74**, 9498–9506.
10. Carrère-Kremer, S., Montpellier-Pala, C., Cocquerel, L., Wychowski, C., Penin, F. & Dubuisson, J. (2002) *J. Virol.* **76**, 3720–3730.
11. Lohmann, V., Korner, F., Koch, J., Herian, U., Theilmann, L. & Bartenschlager, R. (1999) *Science* **285**, 110–113.
12. Pietschmann, T., Lohmann, V., Rutter, G., Kurpanek, K. & Bartenschlager, R. (2001) *J. Virol.* **75**, 1252–1264.
13. Carrasco, L. (1995) *Adv. Virus Res.* **45**, 61–112.
14. Schagger, H. & von Jagow, G. (1987) *Anal. Biochem.* **166**, 368–379.
15. Montal, M. & Mueller, P. (1972) *Proc. Natl. Acad. Sci. USA* **69**, 3561–3566.
16. Kerr, I. D., Dufourcq, J., Rice, J. A., Fredkin, D. R. & Sansom, M. S. (1995) *Biochim. Biophys. Acta* **1236**, 219–227.
17. Aguilera, V. M. & Bezrukov, S. M. (2001) *Eur. Biophys. J.* **30**, 233–241.
18. Andersen, C., Hughes, C. & Koronakis, V. (2002) *J. Membr. Biol.* **185**, 83–92.
19. Neher, E. & Sakmann, B. (1976) *Nature* **260**, 799–802.
20. Hille, B. (1992) *Ionic Channels of Excitable Membranes* (Sinauer, Sunderland, MA).
21. Davies, P. A., Pistis, M., Hanna, M. C., Peters, J. A., Lambert, J. J., Hales, T. G. & Kirkness, E. F. (1999) *Nature* **397**, 359–363.
22. Korngreen, A. & Sakmann, B. (2000) *J. Physiol.* **525**, 621–639.
23. Ewart, G. D., Sutherland, T., Gage, P. W. & Cox, G. B. (1996) *J. Virol.* **70**, 7108–7115.
24. Schubert, U., Ferrer-Montiel, A. V., Oblatt-Montal, M., Henklein, P., Strebel, K. & Montal, M. (1996) *FEBS Lett.* **398**, 12–18.
25. Sunstrom, N. A., Premkumar, L. S., Premkumar, A., Ewart, G., Cox, G. B. & Gage, P. W. (1996) *J. Membr. Biol.* **150**, 127–132.
26. Cordes, F. S., Tustian, A. D., Sansom, M. S., Watts, A. & Fischer, W. B. (2002) *Biochemistry* **41**, 7359–7365.
27. Fischer, W. B., Pitkeathly, M., Wallace, B. A., Forrest, L. R., Smith, G. R. & Sansom, M. S. (2000) *Biochemistry* **39**, 12708–12716.
28. Ma, C., Marassi, F. M., Jones, D. H., Straus, S. K., Bour, S., Strebel, K., Schubert, U., Oblatt-Montal, M., Montal, M. & Opella, S. J. (2002) *Protein Sci.* **11**, 546–557.
29. Piller, S. C., Ewart, G. D., Premkumar, A., Cox, G. B. & Gage, P. W. (1996) *Proc. Natl. Acad. Sci. USA* **93**, 111–115.
30. Melton, J. V., Ewart, G. D., Weir, R. C., Board, P. G., Lee, E. & Gage, P. W. (2002) *J. Biol. Chem.* **277**, 46923–46931.
31. Chizhnikov, I. V., Geraghty, F. M., Ogden, D. C., Hayhurst, A., Antoniou, M. & Hay, A. J. (1996) *J. Physiol.* **494**, 329–336.
32. Sakaguchi, T., Tu, Q., Pinto, L. H. & Lamb, R. A. (1997) *Proc. Natl. Acad. Sci. USA* **94**, 5000–5005.
33. Lin, T. I. & Schroeder, C. (2001) *J. Virol.* **75**, 3647–3656.
34. Mould, J. A., Drury, J. E., Frings, S. M., Kaupp, U. B., Pekosz, A., Lamb, R. A. & Pinto, L. H. (2000) *J. Biol. Chem.* **275**, 31038–31050.
35. Griffin, S. D., Beales, L. P., Clarke, D. S., Worsfold, O., Evans, S. D., Jaeger, J., Harris, M. P. & Rowlands, D. J. (2003) *FEBS Lett.* **535**, 34–38.
36. Hay, A. J., Wolstenholme, A. J., Skehel, J. J. & Smith, M. H. (1985) *EMBO J.* **4**, 3021–3024.
37. Duff, K. C. & Ashley, R. H. (1992) *Virology* **190**, 485–489.
38. Fischer, W. B., Pitkeathly, M. & Sansom, M. S. (2001) *Eur. Biophys. J.* **30**, 416–420.
39. Andersson, U., Butters, T. D., Dwek, R. A. & Platt, F. M. (2000) *Biochem. Pharmacol.* **59**, 821–829.